AD/RHIC-RD-13

Tevatron Beam Position Monitor System

R. Shafer

Los Alamos National Laboratory

2/3/89

Tevatron Beam Position Monitor System.

R. Shafer 8 November 1988
(Rev: 2 February 1989)

Contents

1.	Overall arrangement	page 1.
2.	Beam position monitors	2.
3.	Basic equations for position monitors	4.
4.	Coupling impedance for monitors	5.
5.	Intrinsic monitor resolution	6.
6.	RF Signal processing: AM/PM method	8
7.	Digital signal processing	11.
8.	Beam loss monitor system	12
9.	Communication and timing	14
10.	Typical downloaded parameters	15
11.	Typical encoded triggers on 10 MHz clock	16
12.	Typical self-test features	17
13.	Some typical data readback formats	18
14.	Comments on other beam diagnostics	23
15.	References.	25.

1. Overall Arrangement

1) About 220 beam monitors (110 x, 110 y) around 6280 m circumference. Tune = 19.4, so 5 x and 5 y monitors per betatron wavelength

2) Position monitors are 2 electrode, stripline geometry, 4 kelvin, welded to quadrupoles

3) All electronics is located in 24 Service Buildings, above ground and outside radiation area.

4) Cables to electronics are up to 200 m long.

5) Completely parallel signal processing - no multiplexing of monitors.

6) Electronics is modular: RF electronics in NIM modules.
Digital " in multibus.

7) Local intelligence - Two Ziloq Z80 microprocessors.
PROMs - local storage of programs.
RAM - stores downloaded set parameters.
- stores requested data files.
- stores post-mortem files.

8) Communication - CAMAC serial highway.

9) Beam loss monitor is integral part of system.

2. Beam Position Monitors

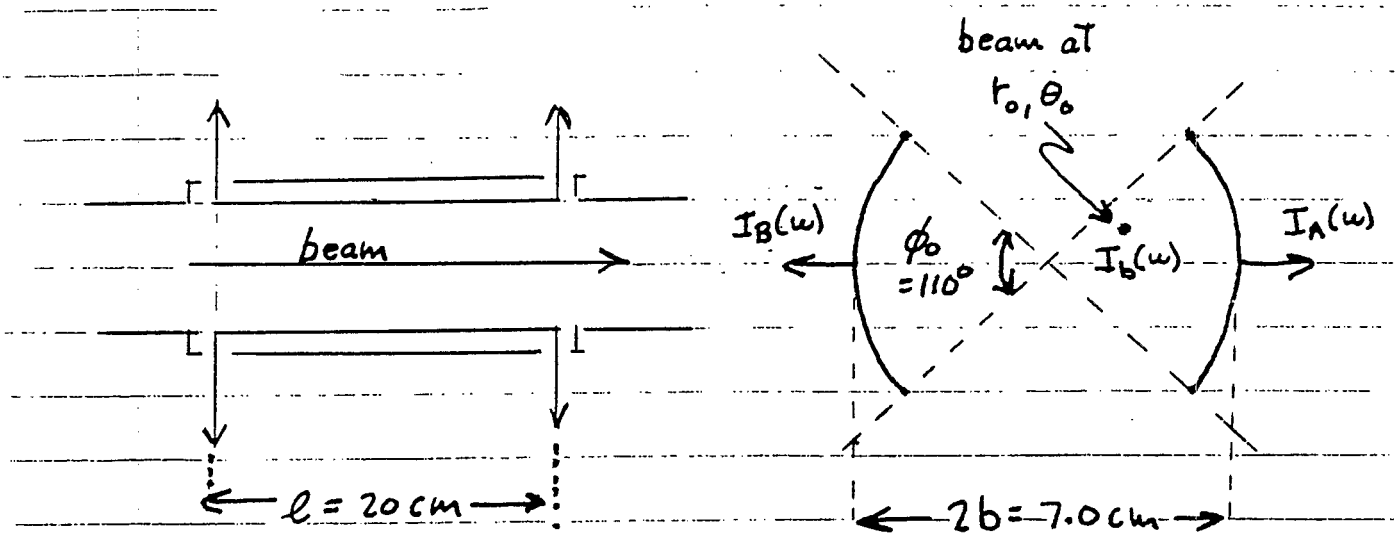

1) Electrodes: 50 ohm transmission lines

2) Very directional when particle velocity = signal velocity

3) Non resonant structure: can calculate ℓ/n.

4) Monitors welded to quadrupoles ($x \rightarrow$ F quad; $y \rightarrow$ D quad)

5) Alignment scheme using wire on quad magnetic axis (Ref 8)

6) All 4 cables brought out through cryostat

7) Coax switches select outputs for p or pbar operation

8) Cables to electronics RG 8 (foam) up to 200 m long.

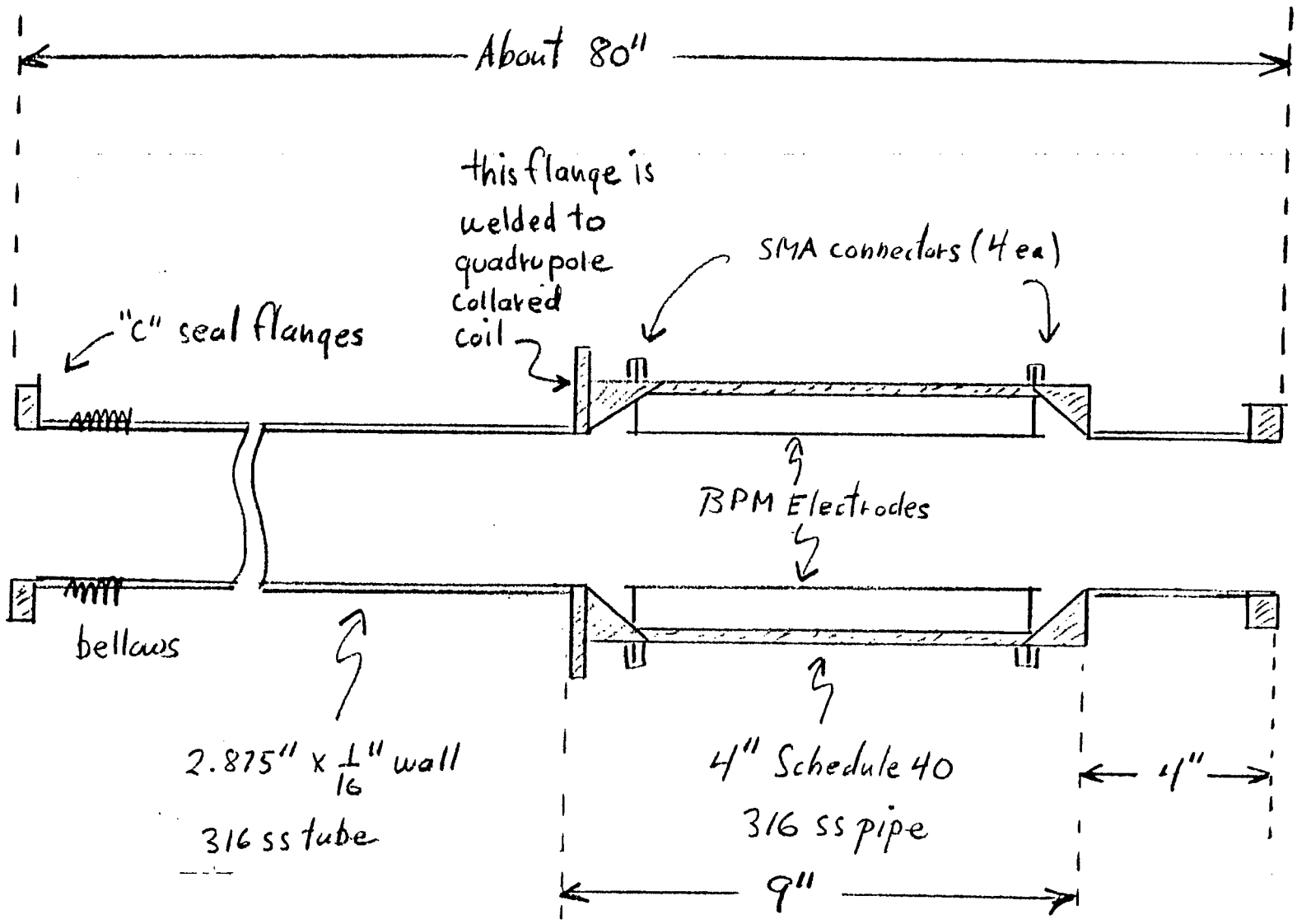

Tevatron Quadrupole Beam Pipe Assembly w/ BPM

9) Major problem

Ceramic in RF connector at 4 kelvin was cracking due to martensitic transformation in 304L stainless steel. Solved by using Cu-Ni alloy - (low yield point)

10) Minor problem

Contact connections in connectors at 4 kelvin not 100% reliable. Only 99.6%.

3. Basic Equations for Beam Position Monitor

1) Assume Gaussian beam bunch (rms bunch length σ)

$$I_b(t) = \frac{eN}{\sqrt{2\pi}\sigma} \exp\left[\frac{-t^2}{2\sigma^2}\right]$$

2) Fourier Transform ($\omega_0/2\pi$ = bunching frequency)

$$I_b(t) = \langle I_b \rangle + 2\langle I_b \rangle \sum_{m=1}^{\infty} I_m \cos(m\omega_0 t)$$

$$\langle I_b \rangle = \frac{eN\omega_0}{2\pi}$$

$$I_b(\omega) = \sqrt{2}\langle I_b \rangle \exp\left[\frac{-m^2\omega_0^2\sigma^2}{2}\right] \quad \text{r.m.s.}$$

3) Pickup signals I_A and I_B : $I_B \leftarrow \left(\quad\right) \rightarrow I_A$

$$I_A = -I_b \frac{\phi_0}{2\pi}\left[1 + \frac{4}{\phi_0}\left(\frac{r_0}{b}\right)\cos\theta_0 \sin\left[\frac{\phi_0}{2}\right] + \cdots\right]$$

$$I_B = -I_b \frac{\phi_0}{2\pi}\left[1 + \frac{4}{\phi_0}\left(\frac{r_0}{b}\right)\cos\theta_0 \sin\left[\pi + \frac{\phi_0}{2}\right] + \cdots\right]$$

this is electrostatic analysis; beam at (r_0, θ_0)

4) Sensitivity S_x for beam displaced distance x in monitor of radius b and electrode angle ϕ_0:

$$S_x = \frac{20}{x}\log_{10}\left(\frac{I_A}{I_B}\right) = \frac{1}{x}\left(\frac{I_A}{I_B}\right)_{dB} = \frac{160}{b\ \ln 10}\,\frac{\sin(\phi_0/2)}{\phi_0}$$

4. BPM Coupling Impedance

1) For electrode pair

$$Z_c(\omega) = \text{Re } Z_c(\omega) + j \,\text{Im } Z_c(\omega)$$

$$= 2 Z_0 \left(\frac{\phi_0}{2\pi}\right)^2 \left[\sin^2\left(\frac{\omega l}{c}\right) + j \sin\left(\frac{\omega l}{c}\right)\cos\left(\frac{\omega l}{c}\right)\right]$$

(derived in Ref. 4) (satisfies Kramers-Krönig relations)

2) Signal power $P(\omega) = I_b^2(\omega)\, \text{Re } Z_c(\omega)$

$$= 2 Z_0 \left(\frac{\phi_0}{2\pi}\right)^2 \sin^2\left(\frac{\omega l}{c}\right) I_b^2(\omega)$$

3) Longitudinal coupling impedance

$$\frac{Z_n(\omega)}{n} = \frac{\text{Im } Z_c(\omega)}{n} = \frac{2 Z_0}{n} \left(\frac{\phi_0}{2\pi}\right)^2 \sin\left(\frac{\omega l}{c}\right)\cos\left(\frac{\omega l}{c}\right)$$

General comments

1) Beam behaves like current source

2) Generally good idea to keep $P(\omega) \geq -40\,\text{dBm}$ (10^{-7} watts) at processing frequency

3) $\frac{Z_n(\omega)}{n}$ inductive at low frequencies, but becomes capacitive at higher frequencies. Wire measurements confirm this.

STRIPLINE BPM IMPEDANCES (LONGITUDINAL)

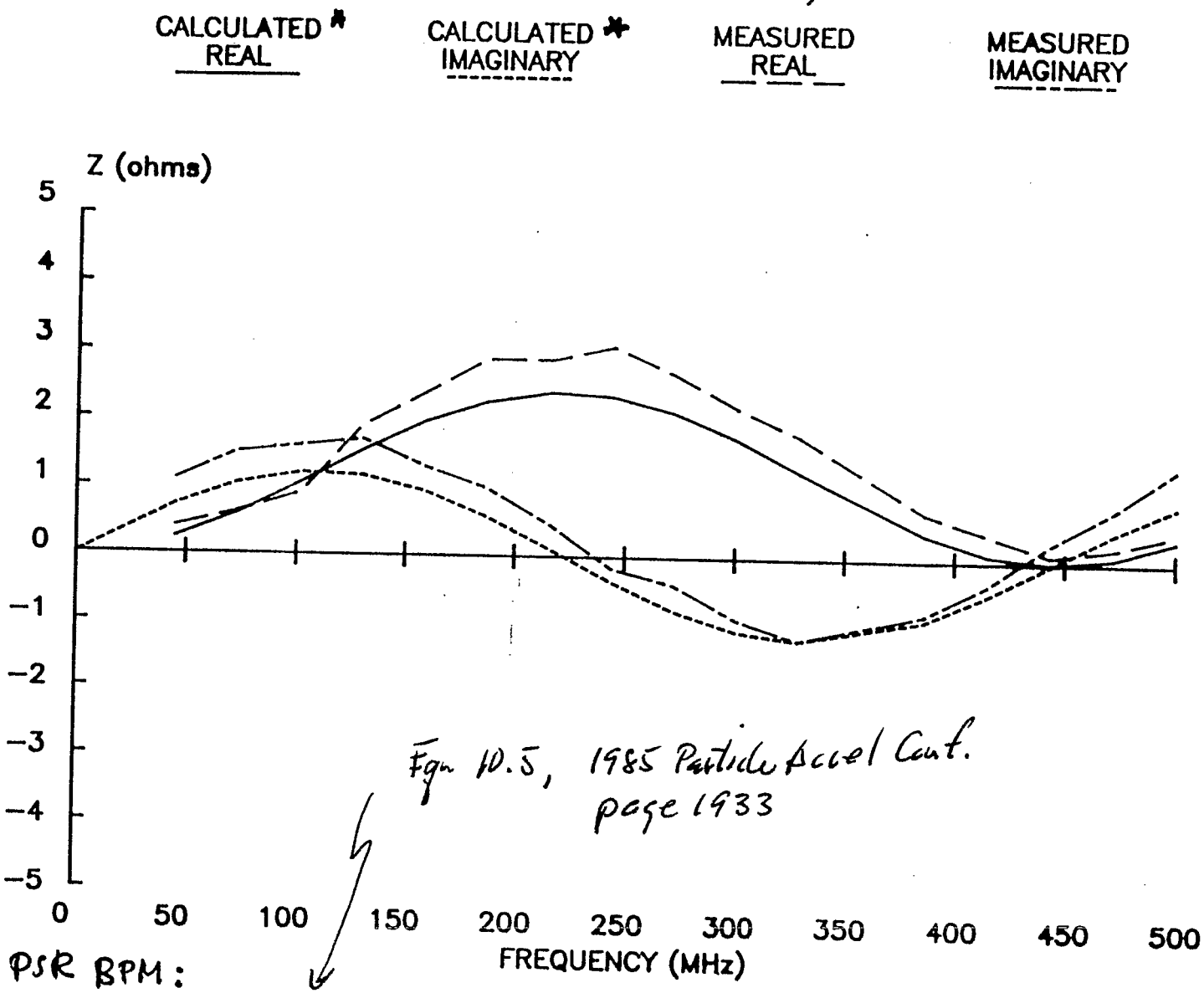

Fgn 10.5, 1985 Particle Accel Conf. page 1933

$\frac{\Phi}{2\pi} = .11$

$l = 33.75c$

$Z_0 = 50\Omega$

4 electrode PSR BPM:

TSD

$$* Z_{11}(\omega) = 4Z_0\left(\frac{\Phi}{2\pi}\right)^2\left[\sin^2\left(\frac{\omega L}{c}\right) + j\sin\left(\frac{\omega L}{c}\right)\cos\left(\frac{\omega L}{c}\right)\right]$$

5. Intrinsic Monitor Resolution

$$\frac{\delta x}{b} \approx \frac{1}{2\sqrt{2}}\sqrt{\frac{P_N}{P_s}}$$ (see Ref 4 eqn 9.1)

P_s = signal power in bandwidth B (per electrode)

P_N = noise power in bandwidth B

= KTB for thermal noise (−114 dBm for B = 1 MHz)

b = monitor aperture radius

Example – HERA-p cold monitor

protons per bunch	10^{10}
bunch frequency	10.4 MHz
bunch length (rms)	$\frac{60\text{ cm}}{4.71 \times 3\times10^{10}} = 0.42$ nsec
Processing frequency	104 MHz
Bandwidth	10 MHz
Amplifier N.F.	3 dB
Pickup ϕ_0	36°
ℓ	40 cm
b	2.8 cm
z_0	50 Ω

$$P_s = z_0\left(\frac{\phi_0}{2\pi}\right)^2 \sin^2\left(\frac{\omega\ell}{c}\right)(N_{ef})^2 \exp\left[-\omega^2\sigma^2\right] = .0753 \text{ mW} = -11 \text{ dBm}$$

$$P_N = -114\text{dBm} + 10\text{dB} + 3\text{dB} = -101\text{dBm}$$

$$\frac{\delta x}{b} = \frac{1}{2.8}(3\times10^{-5}) \simeq 10^{-5} \Rightarrow \delta x \sim 0.3 \text{ microns}$$

this performance is obtainable using Schottky monitor techniques, but not using AM-PM.

For AM-PM circuits add about 20dB noise, so resolution about 10x worse. In addition, if a wide band amplifier is used in circuit prior to limiter, the limiter will be sensitive to the wide-band noise power of amplifier, unless a narrow-band filter is used on amplifier output.

Resolution, Dynamic Range, and Signal to Noise

to obtain a position resolution δx in a pickup with half-aperture b, the ratio of signal power to noise power is:

$$\frac{\delta x}{b} \cong \frac{1}{2\sqrt{2}} \sqrt{\frac{P_N}{P_s}}$$

Ideally, if there is no electromagnetic noise (EMI),

$(P_N)_{dBm} = -114\,dBm \times$ Bandwidth in MHz.

Suppose we had a 100:1 variation in signal amplitude (40dB), a 50mm half aperture and a resolution requirement of 0.1 mm ($\frac{\delta x}{b} = \frac{1}{500} \Rightarrow P_s/P_N = 45dB$), and a noise figure of 20dB. The minimum signal power at full intensity is (assuming no EMI):

KTB (B=10MHz)	−104dBm
noise figure	+ 20 dB
resolution	+ 45
dynamic range	+ 40
Total	+ 1 dBm

6. RF Signal Processing

1) Uses frequency domain amplitude to phase conversion technique (see attached)

Reasons: a) Very fast real-time normalized position signal 5 to 10 RF cycles → 150 micron position precision.

b) Very large dynamic range. Not limited by granularity of digitizers.

c) Signal amplitudes nearly independent of bunch length σ.
In time domain processing (buttons in PETRA) signal amplitude proportional to $1/\sigma^2$.

2) Use proton bunching frequency (53 MHz) for both fixed target and collider operation

3) Narrow band filter at 53 MHz required for collider operation. Use $\lambda/2$ shorted coax. Center frequency matched to 0.1%.

4) AM-PM conversion done using 4 power combiners and 1 90° coax phase delay.

5) Limiters are AM 685 comparators matched to better than ±1° over 50 dB dynamic range.

6) Phase detector is double-balanced mixer.

7) Frequency for processing chosen to be 53 MHz rather than 106 MHz because:

a) Signal amplitude less dependent on σ (bunch length)

b) Limiters work better at lower frequencies

c) More power at longer bunch lengths.

8) Biggest problem areas

a) Matching of Limiters - matched plug-in limiter modules with computer

b) Band pass filters: could not achieve satisfactory matching using lumped components

c) Cables had to be matched to $\pm 5^\circ$ or better.

9) Beam intensity signal uses

a) Homodyne linear detector circuit

b) home-built 3 decade logarithmic amplifier circuit.

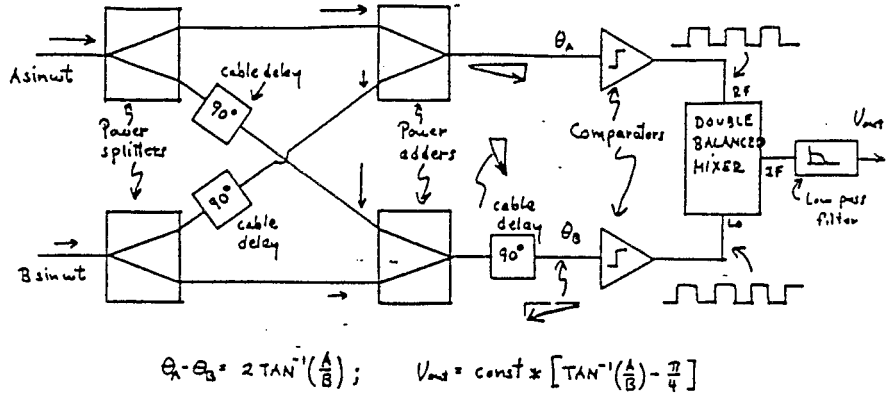

Figure 1. Phasor block diagram of amplitude to phase (AM/PM) circuit.

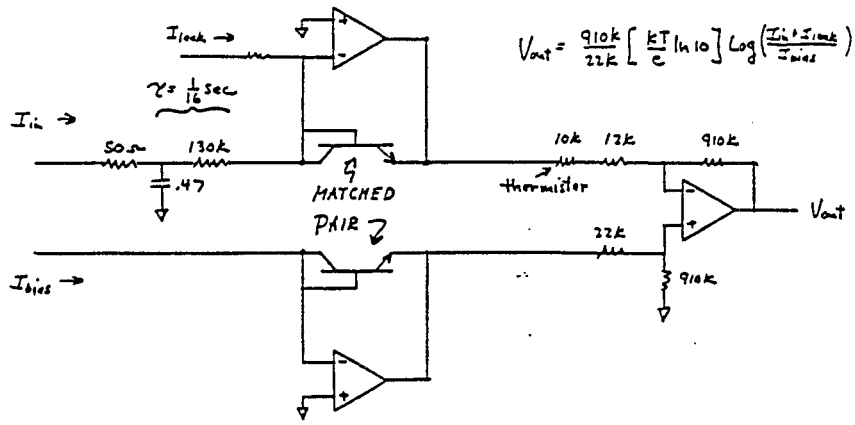

Figure 2. Basic circuit for a four decade integrating logarithmic amplifier.

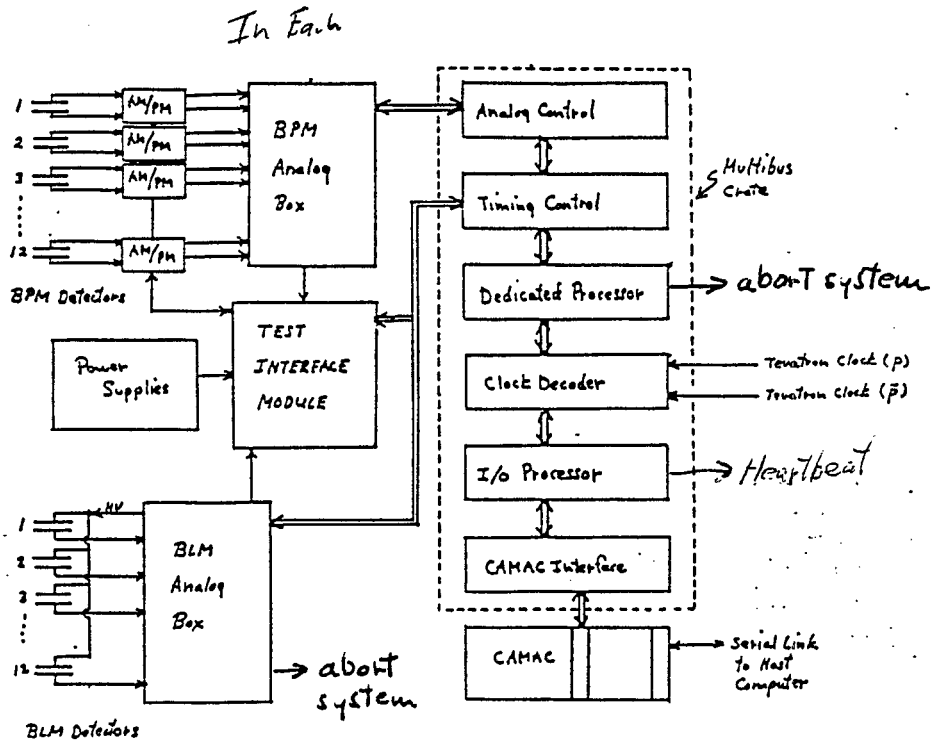

Figure 3. Block diagram of a typical BPM/BLM station.

Neuron-Based Amplitude-to-Phase Converter

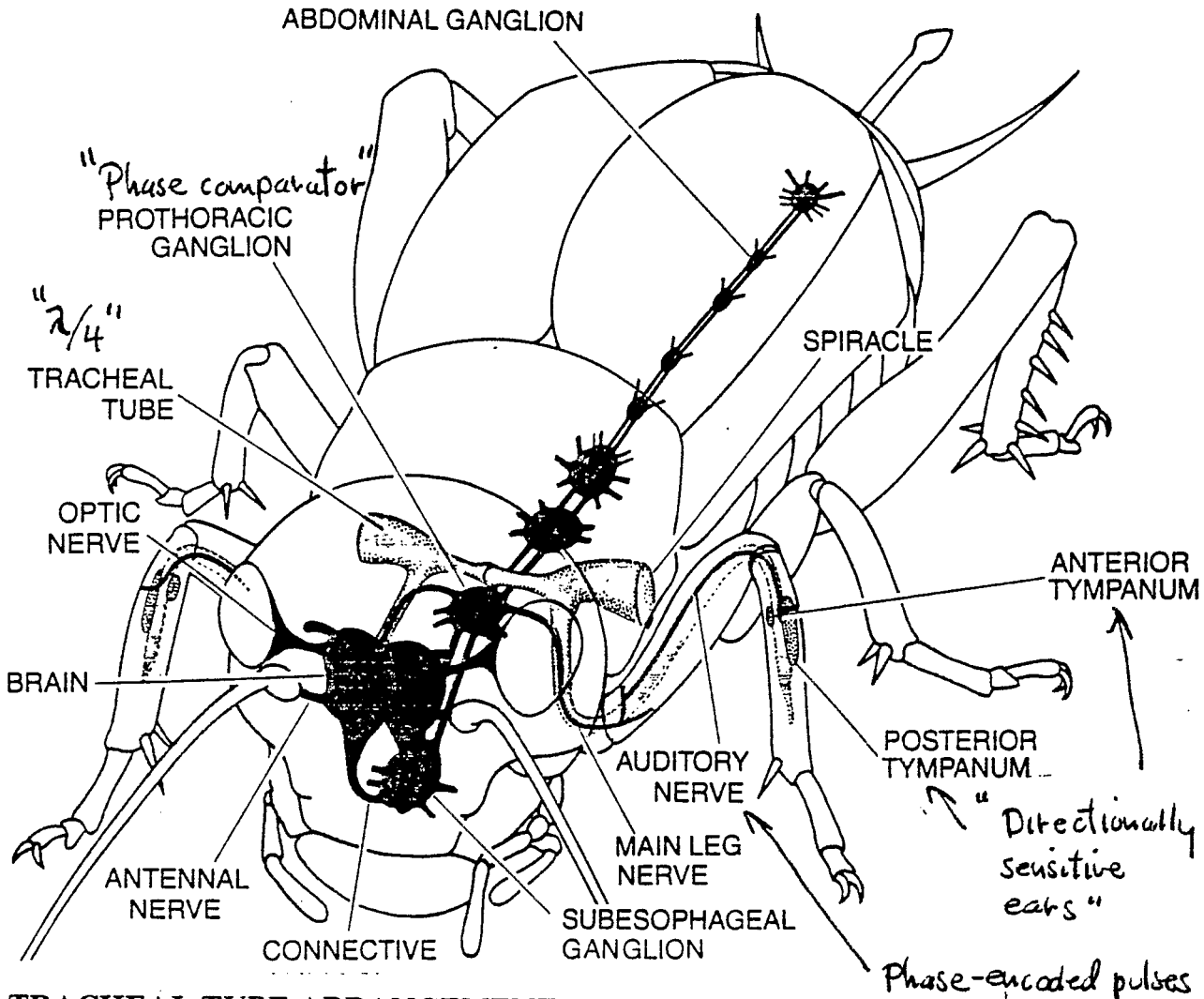

TRACHEAL-TUBE ARRANGEMENT (*blue*) **dominates the cricket's peripheral auditory system. It connects the two "ears," which are curious structures below the knee of each foreleg. On each side of the body a large, funnel-shaped upper branch of the roughly H-shaped tube leads to an opening called a spiracle at the body surface; the tube's lower branch descends through the foreleg to a position between the ear's two tympana, which are auditory membranes overlying an array of receptor cells. Hence sound reaches each ear not only externally, from the enviroment, but also internally, by way of sound pressure within the tracheal tube. The cricket's central nervous system (*red*) consists of a sequence of ganglia (aggregates of neurons), which are linked by pairs of connectives, or bundles of the fibers sent out by the neurons. The frontmost ganglion is the brain, with its optic and antennal nerves. Next comes the subesophageal ganglion, followed by three thoracic ganglia and several abdominal ones. Sensory signals from the array of receptor cells under the auditory tympana enter the prothoracic ganglion, which is the frontmost thoracic ganglion.**

LETTERS

To the Editors:

In "The Federal Support of Mathematics" [SCIENTIFIC AMERICAN, May, 1985], Edward E. David, Jr., has argued convincingly that research and education in mathematics are threatened unless funds are increased substantially in the near future.

Being concerned with the relations between technology and the educational system, we find, however, that this problem (which exists also in other industrialized countries, including our own) has deeper roots. In particular we should like to point out that the general opinion of what mathematics is, and can do, is antiquated and incorrect. Everyone knows there are great opportunities for creative work in both the technical and the natural sciences, but to most people outside the scientific community mathematics appears to be static and sterile. In our opinion this is at least part of the reason it has been difficult to convince politicians and administrators of the importance of mathematics and to attract gifted young people.

The role of elementary education in mathematics in forming most people's concept of the subject is therefore of great importance. If it is true—and we are sure it is—that most pupils leave school with an impression of mathematics as meaningless jiggling around of formulas and proving of obvious statements, financial measures alone will not produce durable results.

It is necessary to develop new educational methods that will allow more people outside the scientific community to appreciate the value of mathematics and to take part in the public debate about its role in society.

JENS BJORNEBOE

GUNHILD NISSEN

Roskilde, Denmark

To the Editors:

The article "Cricket Auditory Communication," by Franz Huber and John Thorson [SCIENTIFIC AMERICAN, December, 1985], describes an auditory-neuron direction-finding system that is remarkably similar in concept to an electronic system developed to measure the position of particle beams in the accelerators at the Fermi National Accelerator Laboratory.

In both systems, the common problem is to measure the relative power of two signals to within a fraction of a decibel when the absolute power levels can vary by 40 or 50 decibels. In the accelerator, passage of the beam between two small electrodes induces signals whose relative amplitudes are directly related to the position of the beam. These two in-phase signals are symmetrically split and recombined in quadrature (that is, with a 90-degree relative phase shift), so that the phase difference of the two resultant output signals varies by about 6.6 degrees per decibel of amplitude difference between the two input signals.

In the cricket, the relative external sound pressure on the two tympana is determined by the orientation of the cricket in relation to its chirping mate. The coupling of the two tympana by the tracheal tube apparently makes the conversion from amplitude to phase. The result is that the relative amplitudes of the two input signals are completely encoded in the relative phase of the two output signals. In the cricket, since there is little useful information in the amplitude of the nerve impulses from the auditory receptors, the omega neurons in the prothoracic ganglia must measure the relative phase of the two nerve signals. This is apparently accomplished by the reciprocal inhibition function in the omega-1 cells by a mechanism similar to that of two cross-coupled monostable multivibrators in an electronic system. The beam-position system differs from this only in that the phase-detection circuit generates an analogue signal proportional to the phase difference with an accuracy equivalent to about a tenth of a decibel in the ratio of the input signals.

The amplitude-to-phase conversion scheme was chosen to measure the beam position as it accomplished the necessary function with a minimal amount of signal processing. It is interesting that genetic selection in the cricket led to a similar result.

ROBERT E. SHAFER

Batavia, Ill.

To the Editors:

I should like to correct a possible wrong impression conveyed in the article entitled "The Search for Proton Decay," by J. M. LoSecco, Daniel Sinclair and me, which appeared in the June 1985 issue of *Scientific American*.

The first publication applying unified gauge-theoretical ideas to the problem of proton decay was by Jogesh C. Pati and Abdus Salam and appeared in *Physical Review Letters* in 1973. This paper marked the beginning of a development of a class of theories that led to the current widespread belief that protons do indeed decay. Following this early work, in 1974 Howard Georgi and Sheldon Lee Glashow discussed the so-called minimal SU(5) theory, putting forward a quantitative prediction of the proton lifetime (which has since been ruled out by the Irvine-Michigan-Brookhaven experiment described in our *Scientific American* article). As we mentioned in our article, long before the advent of a theory, evidence for proton decay was sought by experimentalists. This increasingly stringent series of experiments led William Kropp and me to propose (in mid-1975) a dedicated experiment designed to check proton stability more sensitively.

After we had several long discussions with Salam at the University of California at Irvine, during a visit he made for the express purpose of discussing the experimental status of proton decay, Pati and Salam spoke with officials of the U.S. Department of Energy, urging them to support our proposal. Not persuaded that the problem was worthy of further study (because the existing theory of Pati and Salam gave no firm prediction and the subsequent Georgi-Glashow theory was still numerically vague), they took no action for some time.

Meanwhile my colleagues at Irvine and Case Western Reserve University and I continued to ponder the results we had obtained during the previous decade in the deep South African mine and succeeded in pushing the limits somewhat further. Having held for some 25 years the general belief that conservation laws should be tested experimentally, it was gratifying to me that Pati and Salam had provided a base of a more specific kind and I was anxious to pursue the matter.

The increasingly attractive possibility that a unified gauge theory was compatible with—and even called for—an unstable proton under a wide range of assumptions was considered further by Georgi, Helen R. Quinn and Steven Weinberg, who spearheaded the continuing advance toward a testable quantitative prediction. This development, bolstered by the success of the gauge theory of electroweak interactions, led to a changed climate regarding expanded experimental tests, and the past seven years have seen a burst of activity worldwide.

I hope these remarks will help to clarify the record regarding the seminal contributions of the theorists Pati and Salam to the increasingly central problem of proton decay.

FREDERICK REINES

Irvine, Calif.

2/1/89 10'h

Real-Time Normalized Position Signal

$$V_{out} = V_o \left[\tan^{-1}(A/B) - \frac{\pi}{4} \right]$$

$$\frac{A}{B} = \tan\left[\frac{V_{out}}{V_o} + \frac{\pi}{4} \right]$$

$$\frac{80}{\ln 10} \frac{X}{b} \cong \left(\frac{A}{B}\right)_{dB} = 20 \log_{\text{f}} \left\{ \tan\left[\frac{V_{out}}{V_o} + \frac{\pi}{4} \right] \right\}$$

Real-time normalized position output without need for a division (e.g. $\frac{A-B}{A+B}$).

Normalization prior to digitization reduces dynamic range requirements of digitizer

Log tan function (above) is nearly linear in V_{out}. It is easily linearized after digitization in software using lookup table which converts digitizer counts to displacement in mm.

7. Digital Signal Processing

1) Completely parallel system. One ADC per monitor. Every monitor digitized up to four times per revolution [T = 2 μsec]

2) Sample and hold gate timing based on

   a) Fast self-triggered "beam-present" signal using comparator with computer-set threshold on beam intensity signal (± 10 nsec)

   in combination with

   b) External-clock generated "beam permit" signal. (± 100 nsec)

3) One 8-bit ADC per monitor. Successive approximation with 10 MHz clock. About $30 each.

4) Resolution: Analog, 5 MHz BW ~ 30 microns
   " , few kHz ~ 3 "
   Digital, LSB granularity ~ 150 "

5) Biggest oversight: Inability of digital system to measure very small slow orbit distortions.

6) Non-linear BPM response corrected digitally in host computer.

8. Beam Loss Monitor System

1) Sealed-glass construction; 1 atm pure argon gas; 110 cm^3 active volume.

2) Fast, close-spaced electrode design (2 kV, 1 cm gap)

3) Response — 70 nano Coulombs/Rad
ion collection time ~ 200 microsec
electron " " ~ 1 "

4) Linearity — up to 10 Rads instantaneous — good
" 100 " " — reasonable

5) Leakage current ~ 30 fempto amps at 2 kV

6) 4 decade logarithmic amplifier circuit (1nA to 10μA)

7) Time constant 1/16 sec to match magnet beam-induced quench response (8mW or $\frac{1}{2}$ mJ per gram)

8) Hard-wired (with computer-downloaded threshold settings) into beam abort system.

9) Low maintenance - no circulating gas system

10) Spaced every 30 m around ring (at every BPM).

11) Integral part of BPM system.

12) Beam loss in superconductor to create a quench;

a) instantaneous (< 1/16 sec) $\frac{1}{2}$ mJ/gram or 50 Rads

b) slow (> 1/16 sec) 8 mW/gram or 800 Rads/sec

13) Biggest problems with beam loss monitor

a) Cannot differentiate between Main Ring and Tevatron losses. Main Ring runs at high intensity to create pbars.

b) Non-uniform spacial response along Tevatron. 30m spacing between ion chambers. Located at suspected loss points (i.e. F and D quads) so relatively insensitive to losses in dipoles.

9. Communications and Timing

two communication channels:

1. CAMAC serial highway

a) Point-to-point; host ↔ one of 24 service buildings

b)

host → electronics	parameter downloading
host ← electronics	parameter set verification
host ← electronics	data readback
host → electronics	initiate PROM routines

2. 10 MHz clock with encoded 8 bit trigger events

a) broadcast host → all electronics

b) 256 different trigger events encoded on clock
16 reserved for beam position system using diphase code.

c) Real-time ± 100 nsec

d) Two lines; 1 for protons (clockwise)
1 for pbars (counterclockwise)

10. Typical Downloaded Parameters

1. Beam intensity trigger threshold for "beam present" signal
2. Beam present enable gate delay (0 to 25.6 μsec) and width (0 to 1.6 μsec)
3. Number of averages in multi-turn measurement (8, 16, 32, 64)
4. Repeat time interval of multi-turn averaging (1, 2, 4, 8, 16 msec)
5. Beam alarm and beam abort thresholds for low B field and high B field (four values) for position limits (rarely used) *
6. Same for beam loss monitor limits
7. Beam loss monitor high voltage setting (DAC → DC to DC conv)
8. Multiplicity of beam position or loss monitors to trigger abort.
9. Mask bit to disable all functions of an individual channel
10. Mask bit to disable abort function of individual channel.
11. Select fixed target or collider operation (sets certain delays)
12. Select p or p̄ operation
13. Other similar items

Note: All downloaded parameters are loaded into write/read registers and read back for verification

* Beam position system measured only beam centroids, and was insensitive to beam size. Beam loss monitor was sensitive to beam halo.

11. Typical Diphase-encoded "Events" on 10 MHz Clock

1) Prepare for beam - prevents all self-test routines.

2) End of beam - prohibits beam injection, allows self tests.

3) Reset Clock "T_0".

4) Abort in progress (stops post-mortem FIFO memory).

5) Low B (magnetic) field
6) High B (magnetic) field

} selects abort and alarm threshold settings for position and beam loss limits.

7) Take a single-turn measurement; store in cache RAM.*

8) Store next multiturn measurement in cache RAM.

9) Begin a turn-by-turn measurement.

*cache RAM is a 4 byte memory register readable by CAMAC serial highway.

12. Typical Self-Test Features

All self-test proceedures are stored in local PROMs and carried out under microprocessor control when initiated by host (VAX) computer. Results of tests are stored in RAM for readback by host. Tests can only be initiated when station is in beam-disable mode (beam injection prohibited).

1) Test BPM cable continuity through BPM to 50 Ω back termination

2) Inject 53 MHz RF (0, ± 3dB unbalance) into RF circuit and perform "normal" signal processing

3) Measure all dc power supply voltages

4) Ramp BLM power supply down and up, and perform "normal" signal processing on induced charge in circuit (2 picoFarads x 2 kV = 4 nano Coulombs)

5) Heartbeat (continuous test) - missing pulse triggers abort system etc.

13. Some Typical Data Readback Formats

All readback data stored in RAM for rapid readback by host. Timing of data acquisition (if necessary) controlled by "event" on 10MHz clock..

All Stations

1) Single turn measurement: X position, Y position, intensity, ~~beam~~

2) Multi turn measurement: X position, Y position, beam loss

3) Post Mortem memory - the 512 most recent x and y positions and BLM measurements.

Only 2 Stations

1. Turn-by-turn measurement. One point per turn for both x and y for up to 1024 turns (now ≥ 1,000,000) Signal processing includes Fast Fourier Transform for tune measurements.

Other operations

1. Data archiving for storing data for later comparison to other measurements

2. Display of "difference" plots: (New data vs old data)

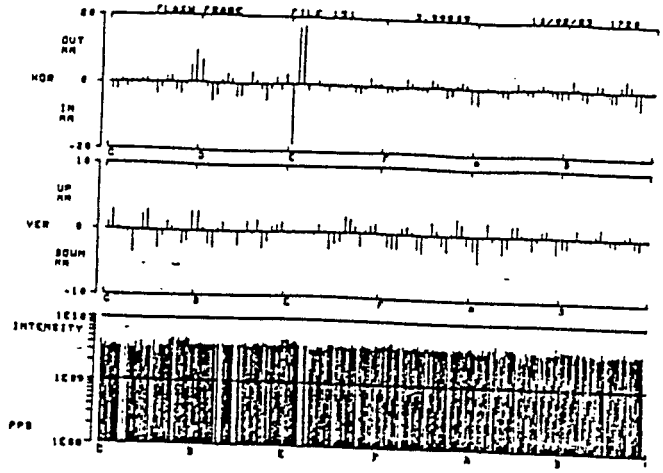

Figure 4. Flash display showing horizontal position, vertical position, and intensity vs. location around the Tevatron for the first turn.

single-turn

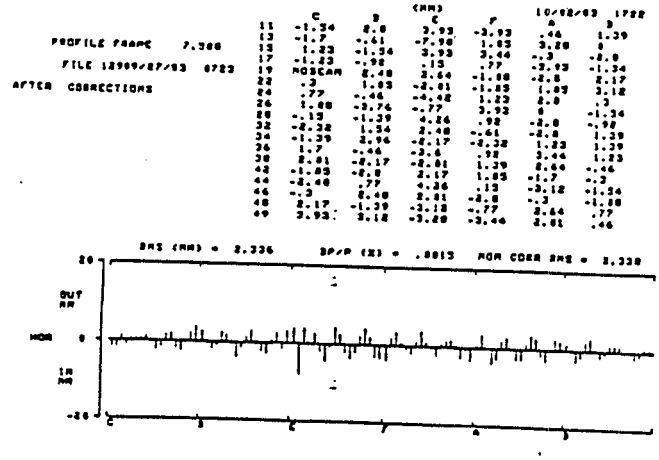

Figure 5. Profile display showing details of the horizontal orbit vs. location around the ring.

multi-turn

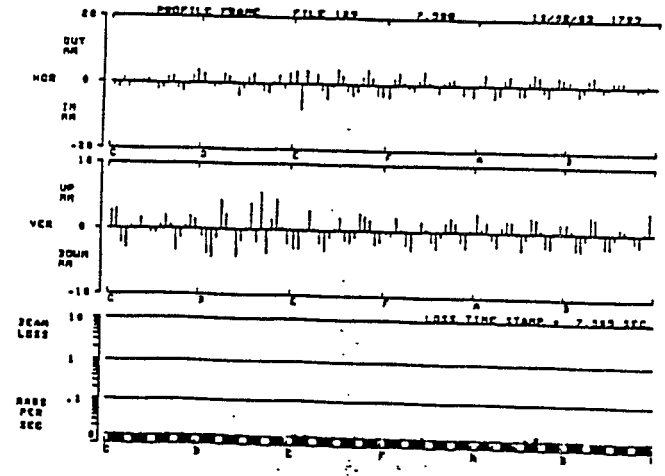

Figure 6. Profile display showing horizontal and vertical orbits, and beam loss vs. location around ring.

multi-turn

Beam

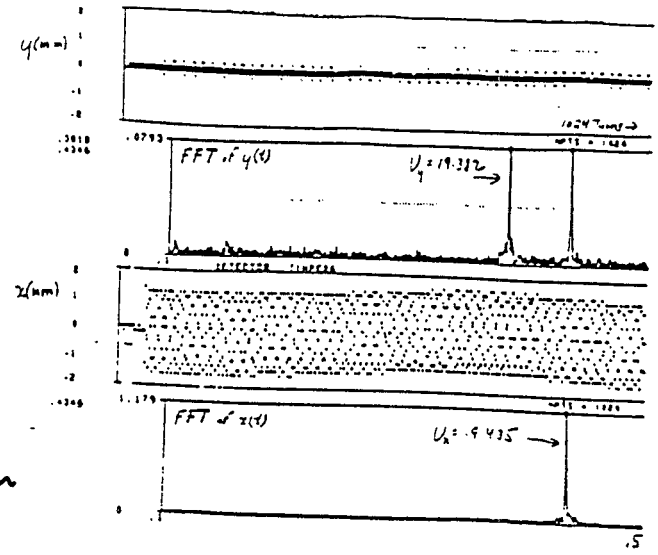

Figure 7. Turn-by-turn plots for "pinged" beam. In this case, the coupling is weak and the tune spread is small. The x and y positions are shown for 1024 turns. The Fast Fourier Transform represents the tune range from 19.10 to 19.50.

1.5 mm kick in x plane. Note the 150 micron LSB resolution in y plane data.

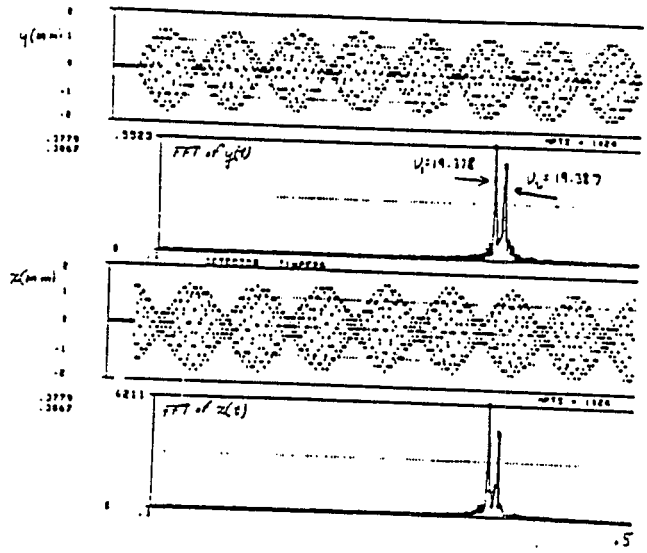

Figure 8. Similar to Figure 7 except that the betatron coupling is strong.

Strong x-y coupling later corrected with skew quadrupoles.

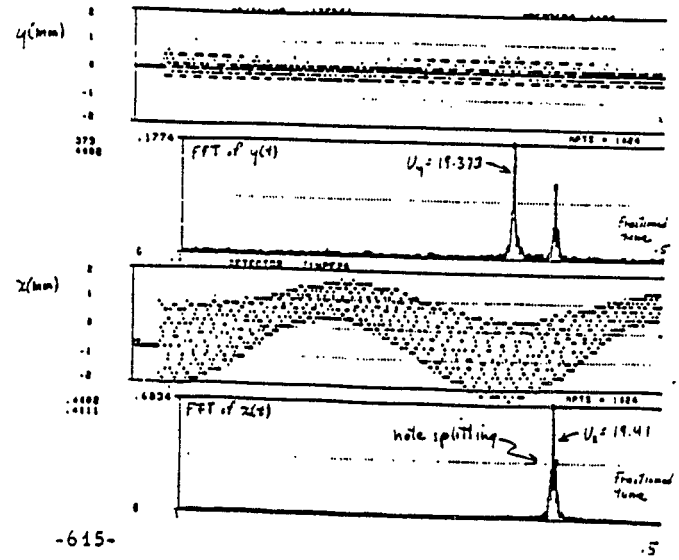

Figure 9. This rather unusual turn by turn plot shows weak coupling between the two betatron modes,

"Snake" due to coherent synchrotron oscillation seen by monitor in dispersive region.

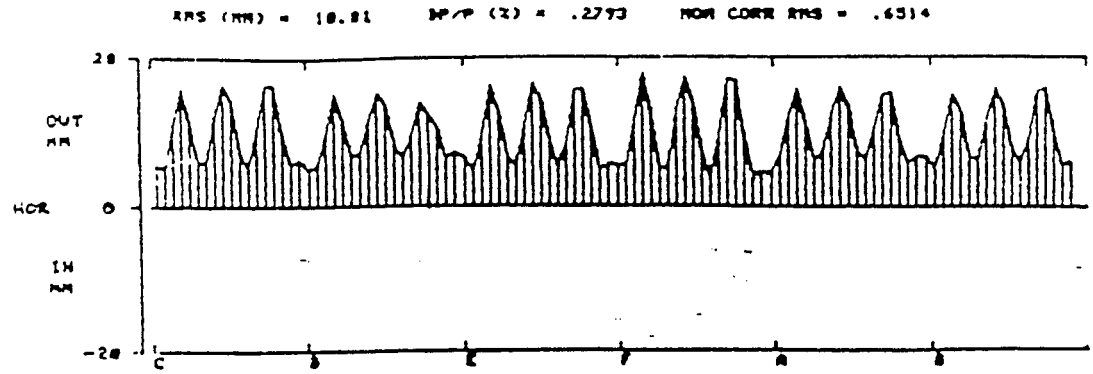

Figure 1. Momentum dispersion measurement with BPM difference plot. The horizontal orbits for two momenta 0.28% apart at 800 GeV are subtracted to show the momentum dispersion around the 6 km circumference. A 16 mm maximum difference in orbits corresponds to a maximum dispersion of about 6 meters.

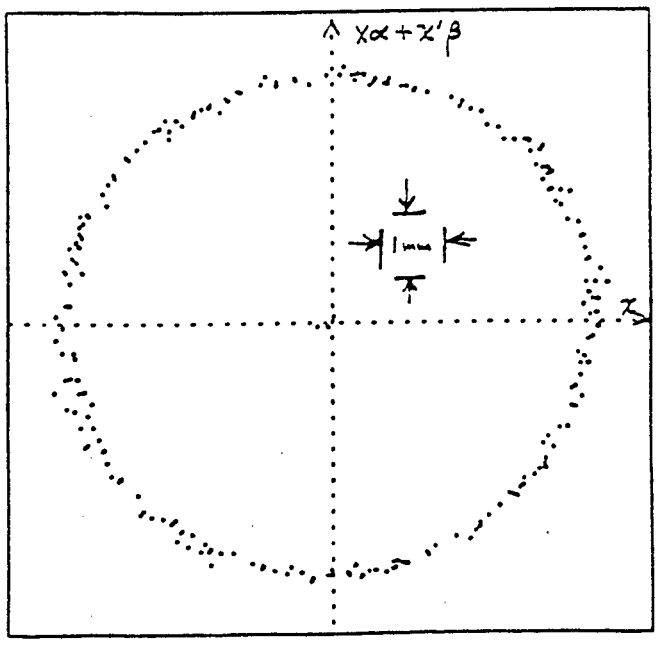

Figure 3. Measured phase space trajectory of coherent horizontal betatron oscillation in Tevatron. Amplitude is about 4 mm. Each point represents one revolution of beam.

(F. Willeke et.al.)

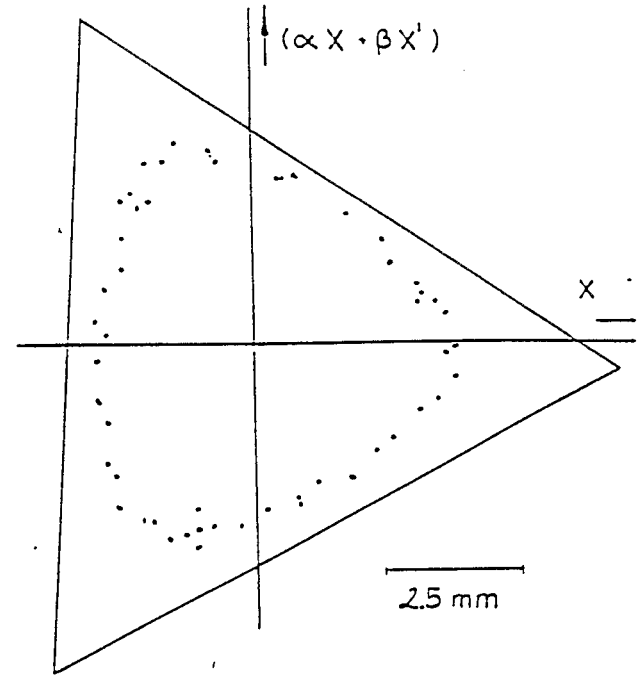

Figure 4. Similar to Figure 3 except that the horizonta tune is near 19.33 and sextapoles have been energized. The triangle represents the calculated limit of stability (separatrices).

600 Gev / Quench at All

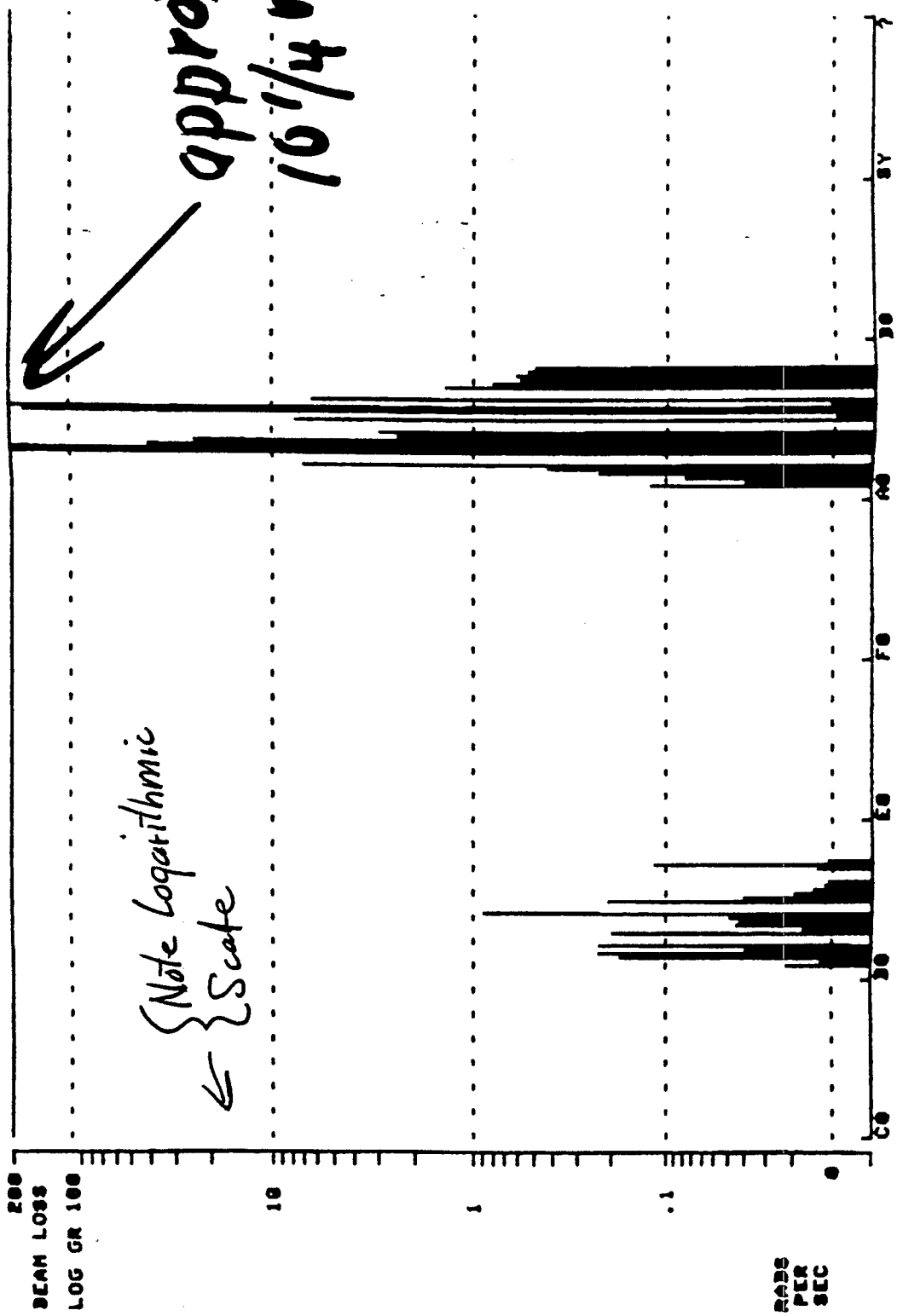

This shows the post-mortem beam loss monitor record for the loss of full beam (10^{13} protons) at 600 Gev due to the failure of the abort system to properly function. 1 kilometer of magnets quenched - no permanent damage.

14. Comments on Other Beam Diagnostics

1. Flying Wire Scanner - best beam profile monitor at Fermi. Invented by Gus Voss, Ewan Paterson, Tom Collins at CEA. Used extensively by Lyn Evans (SPS) and at Fermilab.

2. DCCT (Unser transformer). Good for measuring total circulating current, including protons in wrong RF buckets, or not in any. Hence poor monitor of protons in correct RF bucket.

3. Wide band longitudinal pickup (low coupling impedance)

gap - transit time factor = $\frac{\sin(\omega g/2c)}{(\omega g/2c)}$

set $(\omega g/2c) = 1$ at 5 GHz to minimize gap capacitance

$$g = \frac{2c}{\omega} = \frac{2 \times 3 \times 10^{10}}{2\pi \times 5 \times 10^{9}\ \text{Hz}} = 1.9\ \text{cm}$$ (maximum gap length for 5 GHz)

Make it long enough to see (52 MHz and) 208 MHz isolated bunches; ?

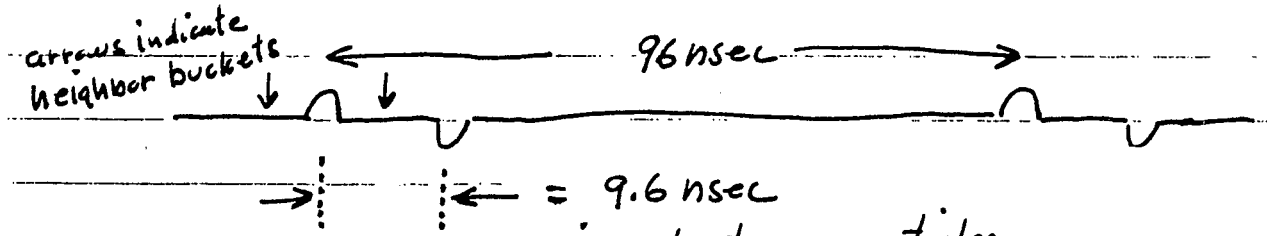

← → = 9.6 nsec
in order to see particles
in neighboring 208 MHz RF buckets

∴ pickup length = 1.44 meters long

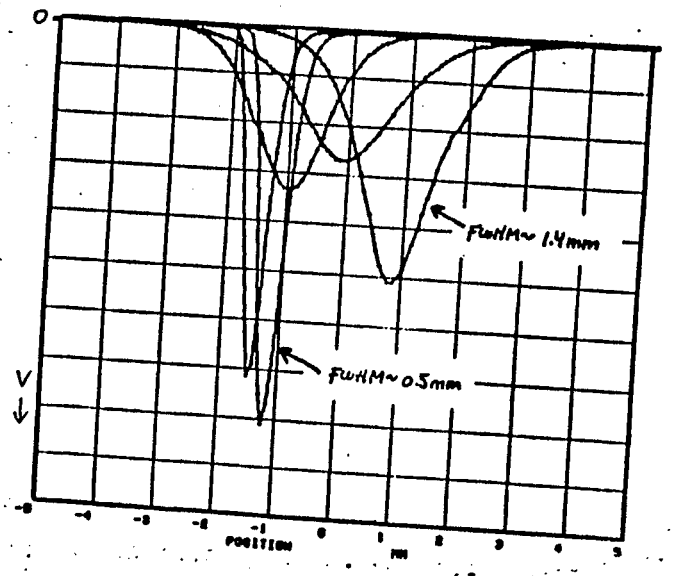

Figure 5. Successive flying wire scans of beam size as the low beta insertion is energized at the B0 collision hall.

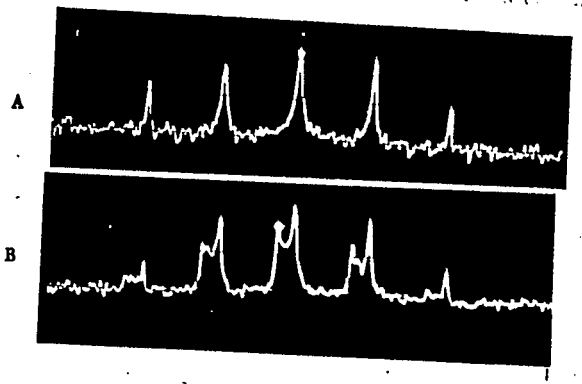

Figure 6. Spectrum analyzer plots showing betatron sideband (center) and synchrotron oscillation satellites displaced at multiples of 38 Hz. Figure 6A shows normal spectrum. Figure 6B shows shift of about 10 Hz caused by ramping Main Ring (about 0.5 m above Tevatron). This corresponds to a tune shift of about 0.0002.

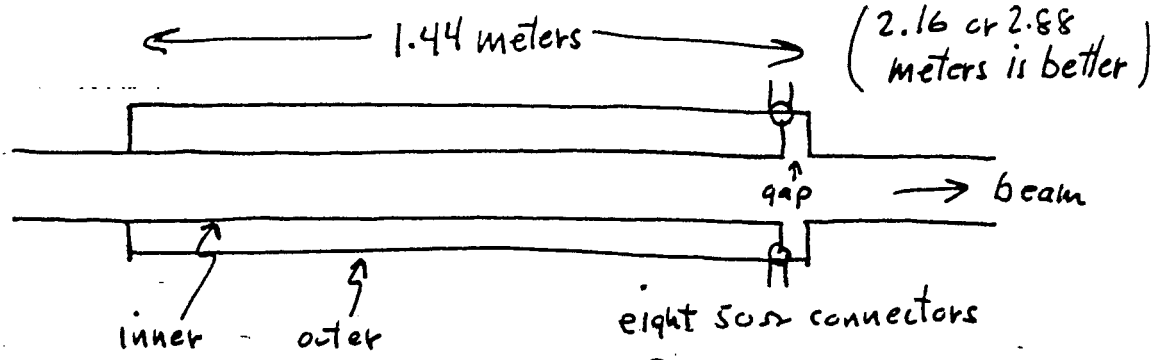

pipe diameter ratio = $\exp\left[\frac{50}{60\times 8}\right] = 1.11$

No ferrite or NZ-51 tiles needed.

4. Shottky monitor. CERN system at 10.7 MHz
Fermi " 21.4

Fermi uses double-down-conversion scheme with phase-locked local oscillators to convert schottky band ($h = 448.5$) to base band

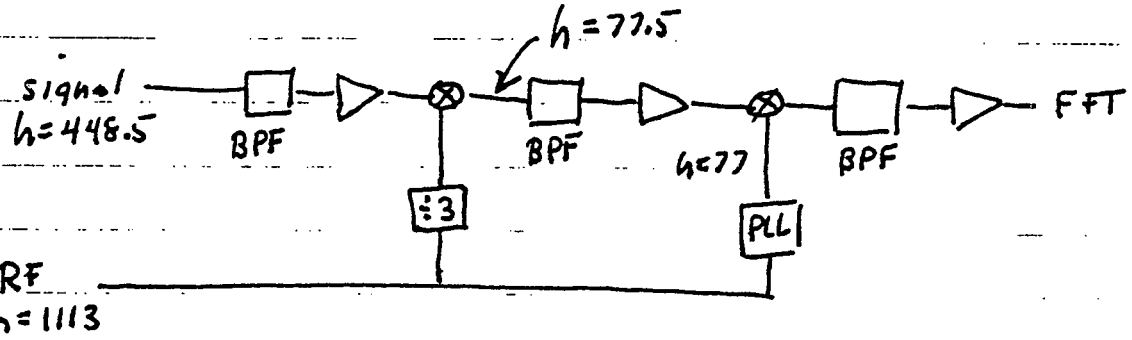

Phase locking local oscillators to RF prevents "drifting" of signal as RF frequency is adjusted. Conversion of schottky band to base band (0 to 47 kHz) allows use of commercial FFT spectrum analyzers.

15. References

1. R. Shafer et. al. Beam Position Monitor
IEEE Trans. Nucl. Sci. 28 pg 2290 (1981)

2. R. Shafer et. al. Amplitude-to-Phase Conversion Circuit
IEEE. Trans Nucl. Sci 28 pg 2323 (1981)

3. R. Shafer et. al. Detailed Description of Tevatron BPM System
Proc. 12th Int. Conf. on High Energy Accelerators
Fermilab (1983) page 609. (Best overall system description

4. R. Shafer Characteristics of Directional Coupler BPMs
IEEE. Trans. Nucl. Sci 32 pg 1933 (1985)

5. R. Shafer Review of Tevatron ~~Etc~~ Beam Diagnostics
IEEE Trans. Nucl. Sci 32 pg 1862 (1985)

Other related papers

6. R. Webber et. al. Beam Monitoring System for Fermilab Booster
IEEE. Trans. Nucl. Sci ? page 541 (1987)

7. R. Webber et. al. Transverse Instabilities in Fermi 200MeV LINAC
1988 LINAC Conf. (Williamsburg)

8. Q Kerns et al. Alignment of BPM's in Tevatron Quadrupoles
IEEE Trans Nucl. Sci. NS-30 page 2250 (1983)